Mon. Not. R. astr. Soc. (1979) **189**, 183–188

Large-scale structure of X-ray clusters of galaxies

P. E. J. Nulsen and A. C. Fabian *Institute of Astronomy, Madingley Road, Cambridge CB3 0HA*

R. F. Mushotzky, E. A. Boldt, S. S. Holt, F. J. Marshall and P. J. Serlemitsos *Goddard Space Flight Center, Greenbelt, Maryland 20771, USA*

Received 1979 March 29

Summary. We use observations from the A-2 experiment on *HEAO-1* to look for very large scale structure (exceeding a degree) in 40 X-ray sources in clusters of galaxies. We find significant evidence for extension only in the relatively nearby Perseus and Virgo clusters. For the remainder of the sources our results place stringent limits on the flux in any very large component.

1 Introduction

Much of the X-ray emission from clusters of galaxies is due to thermal bremsstrahlung of hot intracluster gas (Mitchell *et al.* 1976; Serlemitsos *et al.* 1977) at temperatures $kT \simeq 3$–10 keV (Mushotzky *et al.* 1978; Mitchell *et al.* 1979). Scanning and imaging X-ray observations have been used to determine the gas distribution within a few optical core radii of the cluster centre (Lea *et al.* 1973; Gorenstein *et al.* 1977). Forman *et al.* (1978) have recently reported detection of X-ray emission from an extended region, tens of optical core radii in size, around each of eight clusters of galaxies. This could indicate that a large mass of hot gas occurs at these distances and would be an important consideration in the study of clusters of galaxies.

We have used the A-2 experiment on *HEAO-1* to observe 40 X-ray emitting clusters of galaxies including the eight with reported large-scale emission. We find that extended X-ray emission similar to that reported by Forman *et al.* (1978) is not a general property of clusters of galaxies.

2 The observations and analysis

The A-2 experiment (a collaborative effort led by E. Boldt of GSFC and G. Garmire of CIT, with collaborators at GSFC, CIT, JPL and UCB) on *HEAO-1* (Rothschild *et al.* 1979) consists of six multiwire gas proportional counters pointing perpendicular to the spin axis of the spacecraft. Each of the detectors is collimated with two co-aligned fields of view having different widths in the scan direction. The medium-energy detector, MED, (3.2–7 keV above 30 per cent peak efficiency) and high-energy detector 3, HED3, (3–15 keV above 30 per cent peak efficiency) both have a 3° x 3° and a 3° x 1°.5 field of view.

Scanning data for each of 40 clusters of galaxies, including all those studied by Forman *et al.* (1978), were combined into bins 3° x 0°.25 perpendicular to, and parallel to, the scan path, respectively. The count rate for each cluster was then determined by least-squares fitting a point source with constant background to the binned data. The effect of binning

Table 1. Fitted count rates in the detectors for the 40 cluster X-ray sources. The count rates in the 3° X 1°.5 detectors have been multiplied by the ratio area (3°)/area(1°.5) = 1.0763 and 1.0388 for the MED and HED3 respectively. The differing areas are due to collimator obscuration. The eight sources of Forman *et al.* are marked by an asterisk. The sources are listed in order of increasing count rate.

Cluster	MED 3°x3° (ct s^{-1})	MED 3°x1°.5 (ct s^{-1})	HED 3°x3° (ct s^{-1})	HED 3°x1°.5 (ct s^{-1})
A400	0.23±0.12	0.30±0.14	0.11±0.11	0.06±0.10
A140	0.28±0.10	0.40±0.11	0.39±0.09	-0.14±0.09
Klemola 44	0.37±0.14	0.44±0.17	0.28±0.10	0.21±0.11
A2312	0.41±0.11	0.32±0.13	0.29±0.11	0.42±0.12
A1904	0.29±0.08	0.39±0.09	0.45±0.08	0.41±0.09
*A2657	0.43±0.12	0.50±0.14	0.29±0.10	0.42±0.11
*A576	0.45±0.08	0.42±0.09	0.37±0.09	0.42±0.10
A2204	0.38±0.09	0.40±0.10	0.45±0.07	0.43±0.08
A644	0.32±0.10	0.57±0.12	0.36±0.08	0.52±0.09
*A2589	0.38±0.14	0.48±0.17	0.45±0.13	0.47±0.14
A1367	0.48±0.12	0.59±0.14	0.41±0.09	0.51±0.10
*A2666	0.41±0.10	0.72±0.12	0.37±0.09	0.54±0.10
A2440	0.58±0.14	0.52±0.16	0.54±0.10	0.62±0.11
CA0343-536	0.59±0.12	0.37±0.13	0.76±0.11	0.70±0.12
A2065	0.76±0.10	0.55±0.12	0.68±0.09	0.44±0.10
SC0316-443	0.65±0.13	0.51±0.15	0.74±0.10	0.95±0.11
A119	0.74±0.07	0.80±0.09	0.75±0.05	0.71±0.04
A496	1.06±0.14	0.87±0.16	0.81±0.11	0.84±0.12
A1060	0.99±0.09	1.11±0.11	0.84±0.08	0.78±0.09
A85	0.94±0.11	1.05±0.13	1.08±0.09	0.91±0.10
A2147	1.01±0.13	1.15±0.16	1.07±0.11	0.89±0.11
A478	0.98±0.13	0.87±0.16	1.22±0.10	1.26±0.12
*A401	1.17±0.12	0.93±0.14	1.37±0.09	0.95±0.10
Sersic 0430-615	0.82±0.13	1.37±0.15	0.85±0.13	1.55±0.15
*A1795	1.32±0.13	1.38±0.15	1.04±0.11	1.17±0.12
*SC0626-541	1.44±0.12	1.21±0.14	1.52±0.11	1.39±0.12
*A2142	1.28±0.13	1.15±0.15	1.61±0.10	1.50±0.11
A2256	1.33±0.09	1.38±0.11	1.41±0.10	1.50±0.11
SC2009-569	1.38±0.09	1.39±0.12	1.58±0.10	1.48±0.11
SC1344-325	1.61±0.09	1.52±0.11	1.67±0.09	1.18±0.10
A2199	1.48±0.12	1.55±0.14	1.37±0.11	1.63±0.12
A2029	1.84±0.13	1.10±0.15	1.77±0.10	1.36±0.11
SC1326-311	1.60±0.11	1.58±0.13	1.70±0.10	1.60±0.11
SC1251-290	1.88±0.14	1.61±0.16	1.81±0.11	1.81±0.12
A754	1.81±0.16	1.46±0.17	2.12±0.12	1.82±0.15
Centaurus	2.33±0.11	2.12±0.13	2.50±0.10	2.29±0.11
A2319	2.74±0.10	2.92±0.13	3.37±0.10	3.53±0.11
Coma	5.60±0.14	5.73±0.18	6.24±0.12	6.11±0.15
Virgo	7.63±0.17	6.85±0.22	6.48±0.12	5.90±0.15
Perseus	13.98±0.12	13.31±0.16	15.56±0.10	14.99±0.12

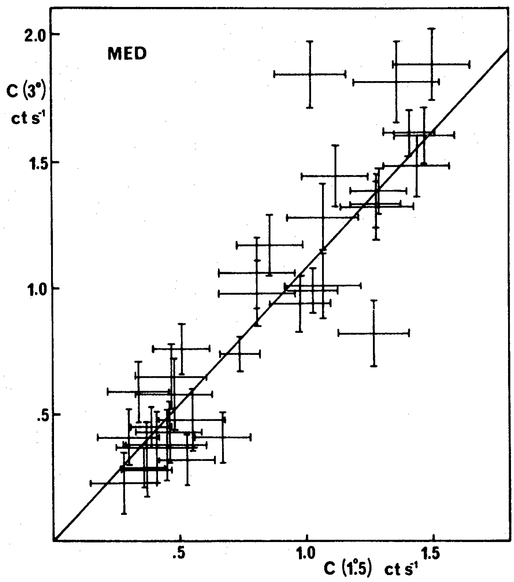

Figure 1. The count rate measured in the 3° × 3° detectors plotted against that in the 3° × 1°.5 detectors for the MED. The full line is the expected locus for a point source (slope = 1.0763 = area (3°)/area (1°.5)). The error bars are plus and minus 1σ.

was allowed for in the point-source response of the collimators. The resulting count rates together with 1σ errors (obtained from the fitting procedure assuming photon statistics) are listed in Table 1, with sources ranked in order of increasing count rate, and are plotted for the MED in Fig. 1.

An extended source will in general give a greater count rate in the 3° collimators than in the 1°.5 collimators. In Fig. 2 we plot the residuals:

$$R_i = C_i(3°) - C_i(1°.5),$$

where $C_i(3°)$ and $C_i(1°.5)$ are the count rates for the ith source from Table 1. The sources are again ranked in order of increasing count rate C. The only sources showing marginally

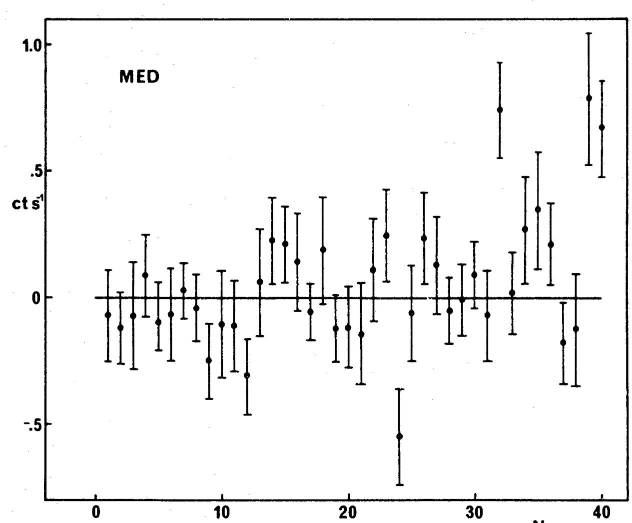

Figure 2. The residuals (see definition in the text) with 1σ error bars for each of the 40 sources plotted against the source number for the MED. The sources have been ranked in order of increasing count rate. A positive residual is expected for large extended sources. The three sources showing marginally significant excesses are A 2029, Virgo and Perseus.

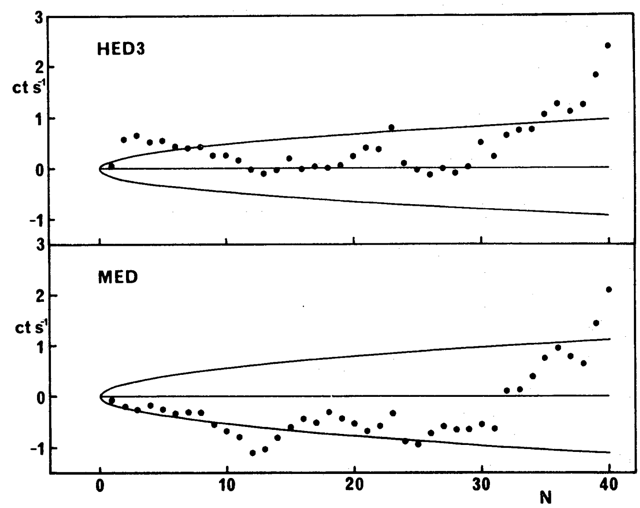

Figure 3. The sums of the residuals for the first N sources versus N, with sources ranked in order of increasing count rate. The solid curves show the cumulative 1σ errors about zero. The upturn over the last 10 sources is largely due to A 2029, Virgo and Perseus.

significant excesses in their 3° fluxes are A 2029, Virgo and Perseus. The excess in A 2029 is probably due to confusion with NGC 5920 (2A 1519+082). Inspection of the data shows that the excesses for Perseus and Virgo are due to extension of these relatively nearby sources. There is no measurable excess for the Coma cluster.

A major source of error in the fitted count rates is the non-uniformity of the X-ray background. The background fluctuations in the effective 3° x 1°.5 difference between the 3° x 3° and 3° x 1°.5 beams are roughly 5 per cent (Fabian 1975; Shafer *et al.* 1978). The 3° x 1°.5 background in the MED is typically 2.8 ct/s per bin and thus the fluctuations are of order 0.14 ct/s per bin. Since the bins overlap, this gives an estimate of the error in the count rates which is comparable with the photon noise errors found from the fitting procedure.

Source confusion and background fluctuations produce correlated errors in different measurements of the same source. We have therefore combined the residuals from many different sources in order to reduce these errors.

A systematic excess was searched for in the summed residuals. The results are shown in Fig. 3. The upturn over the last 10 sources is almost entirely due to A 2029, Virgo and Perseus. (The sums of the residuals for these sources are 2.2 ct/s and 1.6 ct/s in the MED and HED3 respectively.) In any case we expect an upturn in the sum for the nearby resolved, and thus brighter sources. To avoid these we take a result for the first 30 sources only. The sums of the residuals are -0.56 ± 0.97 ct/s and 0.49 ± 0.82 ct/s (1σ errors) for the MED and HED3 respectively. Thus the ratio of the 3° to 1°.5 fluxes for the MED is 0.976 ± 0.046 and for HED3 is 1.022 ± 0.036.

The summed residuals for the eight clusters studied by Forman *et al.* (1978) are 0.10 ± 0.5 ct/s and 0.17 ± 0.4 ct/s for the MED and HED3 respectively. (A 401 shows a 2.5σ excess in HED3.) These translate to 3° x 3° to 3° x 1°.5 ratios of 1.015 ± 0.07 and 1.025 ± 0.06, respectively.

3 Interpretation

The above results may be compared with the count rates expected from various X-ray profiles. The expected flux ratios from a rectangular profile of width $2a$ in the scan direction, and from a simple isothermal gas sphere with volume emissivity varying as $(1+r^2/a^2)^{-3/2}$ (to

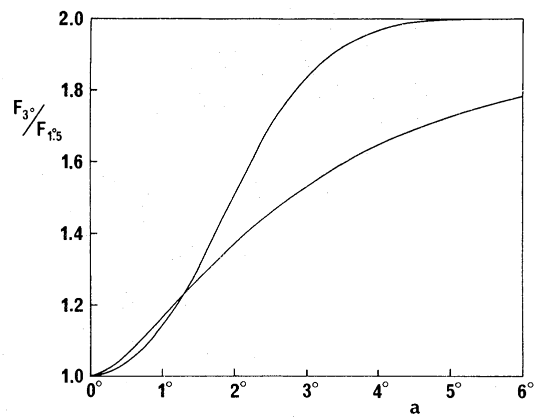

Figure 4. The expected 3° X 3° to 3° X 1°.5 flux ratios as a function of source size for (1) a source with a rectangular line profile and half-width a (upper curve on the right) and (2) a source where surface brightness varies radially as $(1+r^2/a^2)^{-5/2}$ (cf. Forman *et al.* 1978). In both cases the ratio approaches 2 for $a \gg 3°$. We note that the estimated ratios are similar for $a \sim 1°$.

compare with Forman *et al.* 1978), are shown in Fig. 4. Our 97 per cent upper limits on a for the latter distribution are 1°.30 (MED) and 1°.05 (HED3) from the summed residuals of the eight clusters, and 0°.55 (MED) and 0°.65 (HED3) for the 30 weaker clusters (which include the above eight and have a similar range of distances).

We have tested the hypothesis that the X-ray sizes determined by Forman *et al.* (1978) for the eight clusters are consistent with our results. The reported angular sizes, a, lead to predicted summed residuals of 1.27 ± 0.06 ct/s (MED) and 1.25 ± 0.05 ct/s (HED3), after due allowance has been made for the collimator scanning function. Comparison with our measured residuals enables us to reject the hypothesis at the 99 and 99.5 per cent confidence limits for the MED and HED3 respectively. Our results are consistent with no large-scale extension.

We note that we are comparing count rates from the same detector, the only difference being the collimator structure which defines the 3° x 3° and 3° x 1°.5 fields of view. In determining X-ray count rates we have used our best-fitting positional centroids, which are located with an error much less than the collimator size (i.e. to < 0°.3). It is not clear that the peak X-ray emission should coincide with the optical centre of a cluster, and source identifications have usually been made if these positions are within ~0°.5 of each other (Jones & Forman 1978; McHardy 1978). This positional uncertainty could lead to an underestimate of the source luminosity when a collimator of comparable size is used, and is also a component of the uncertainty in the count rate. This effect need not apply in the case of stellar objects, or active galaxies, for which a precise location is known.

4 Discussion

We find no evidence in our data to support the large extensions around the clusters of galaxies reported by Forman *et al.* (1978). We limit the angular extension on 30 clusters to less than 0°.55 (MED) and 0°.65 (HED3) after combining the data. A more complex X-ray distribution and/or spectral behaviour than has hitherto been considered is necessary before our results can be brought into agreement with those of Forman *et al.* (1978).

Our observations provide constraints on the amount of X-ray emitting gas away from the cores of clusters of galaxies. Such limits are model dependent, and will vary, for example, with the assumed polytropic index and galaxy distribution. We leave detailed analysis to a later paper (Nulsen *et al.*, in preparation).

Acknowledgments

We thank Dr R. Mitchell for helpful comments. PEJN is grateful to Dr E. Boldt and his colleagues at Goddard Space Flight Center for their hospitality, and acknowledges the Institute of Astronomy, a Hackett Studentship from the University of Western Australia and an Isaac Newton Studentship for financial support. ACF thanks the Radcliffe Trust for support.

References

Fabian, A. C., 1975. *Mon. Not. R. astr. Soc.*, **172**, 149

Forman, W., Jones, C., Murray, S. & Giaccconi, R., 1978. *Astrophys. J.*, **225**, L1.

Gorenstein, P., Fabricant, D., Topka, K., Tucker, W. & Harnden, F., 1977. *Astrophys J.*, **216**, L95.

Jones, C. & Forman, W. 1978. *Astrophys J.*, **224**, 1.

Lea, S. M., Silk, J., Kellogg, E. & Murray, S. S., 1973. *Astrophys. J.*, **184**, L105.

McHardy, I., 1978. *Mon. Not. R. astr. Soc.*, **184**, 783.

Mitchell, R. J., Culhane, J. L., Davison, P. J. N. & Ives, J. C., 1976. *Mon. Not. R. astr. Soc.*, **175**, 29P.

Mitchell, R. J., Dickens, R. J., Bell Burnell, S. J. & Culhane, J. L., 1979. *Mon. Not. R. astr. Soc.*, in press.

Mushotzky, R. F., Serlemitsos, P. J., Smith, B. W., Boldt, E. A. & Holt, S. S., 1978. *Astrophys. J.* **225**, 21.

Rothschild, R., Boldt, E., Holt, S., Serlemitsos, P., Garmire, G., Agrawal, P., Riegler, G., Bowyer, S. & Lampton, M., 1979. To be published.

Serlemitsos, P. J., Smith, B. W., Boldt, E. A., Holt, S. S. & Swank, J. H., 1977. *Astrophys. J.*, **211**, L63.

Shafer, R. A., Boldt, E. A., Holt, S. S., Serlemitsos, P. J. & Rothschild, R. E., 1978. *Bull. Am. astr. Soc.*, **10**, 502.